

DEVELOPMENT OF A SYSTEM TO INVERT EDDY-CURRENT

DATA AND RECONSTRUCT FLAWS*

L. David Sabbagh and Harold A. Sabbagh
Analytics, Inc.
2634 Round Hill Lane
Bloomington, IN 47401

THE PROBLEM

In this report we describe an approach to the reconstruction of flaws, not merely their detection. This will give us the ability to obtain much more information about the nature of the flaw. By "flaw" we mean virtually any departure of the medium from a standard condition, which is known a priori, such as may be produced not only by a crack but also by conductivity in homogeneities produced by stresses, magnetite build-up, etc. Our approach is very much in the spirit of contemporary work in inverse methods in electromagnetics [1-3] and electromagnetic-geophysical prospecting [4-11].

The method of solving this problem is based on minimizing the square of the error between the actual measured data and that produced by the model-system, the model-output (this error is often called the residual). The parameters that are varied to produce the optimum model, in the least-squares sense, are, of course, the conductivities that are assigned to each cell in the mesh of Figure 1.

Thus, mathematically, we wish to determine a set of unknown parameters σ_j , $j=1, \dots, M$, where M is the number of cells in the mesh, from a set of data, e_i , $i=1, \dots, N$, where e_i are the voltages induced into the N sensing coils. The e_i are functionally related to the σ_j in a known way; that is

*This work was supported by the Naval Surface Weapons Center (Code R34), White Oak Labs, Silver Spring, MD 20910, under Contract No. N60921-81-C-0302.

$$e_1 = f_1(\sigma_1, \dots, \sigma_M) \quad (1)$$

$$e_2 = f_2(\sigma_1, \dots, \sigma_M)$$

.

.

.

$$e_N = f_N(\sigma_1, \dots, \sigma_M)$$

Hence, given the σ_j we can calculate the e_i by treating this as a "forward" problem. The equations (1) that define the forward problem are determined by using electromagnetic theory.

But it is the voltages, e_i , that are the given data, so we must invert the system, (1), to determine the σ_j . We do this by minimizing the error function

$$F(\sigma_1, \dots, \sigma_M) = \left[\sum_{i=1}^N (e_i - f_i)^2 \right]^{1/2} \quad (2)$$

Iterative methods are commonly used to carry out the minimization of (2). The iterative method successively improves a current model, i.e., a current estimate of the σ_j , until the error measure, (2), is small and the parameters are stable with respect to reasonable changes in the model.

The success of this method of inversion depends largely on the availability of suitable numerical algorithms for carrying out the least-squares solution of (1). Any algorithm chosen must contend with the fact that the problem as posed in (1) and (2) is generally quite ill-conditioned, which means that small variations in input data can produce quite large variations in the solution. The commercially available FORTRAN packages, LINPACK [12] and MINPACK [13], contain well-written codes for least-squares algorithms, and these codes served as the basis of the numerical experiments to be described in this report. LINPACK consists of linear equation-solving algorithms, and MINPACK contains nonlinear least-squares algorithms.

These experiments indicate that the inversion method works quite well on simulated flaws, even when the data is corrupted by as much as 20%; this is quite important in applications. Another nice feature is that once the nonlinear inversion algorithm has converged, it is possible, using the techniques of linear inverse theory, to assess the errors and resolution in the estimate of the final model. The objective is to determine which features of the model are well-resolved and important to the interpretation of the data and which

features are irrelevant, in the sense that the data neither support nor reject their inclusion in the model. This is also quite useful in eddy-current NDE.

THE MODEL

We introduce the following notation

$E_{1,2}(r, z)$ = Electric field in region 1 or 2, with flaw present

$E_0(r, z)$ = Electric field with flaw absent, due to exciting coil.

Then we have the following basic integral equation for computing E in the flawed region, which is in region 2:

$$E_2(r, z) + j\omega\mu_0\sigma_0 \iint_{\text{Flaw}} G_{22}(r, z; r', z') E_2(r', z') \left(\frac{\sigma_f}{\sigma_0}(r', z') - 1\right) r' dr' dz' = E_0(r, z) \quad (3)$$

In addition, we have the integral relation for computing the perturbed electric field at the probe coil (which lies within region 1):

$$(E_0 - E_1)(r, z) = j\omega\mu_0\sigma_0 \iint_{\text{Flaw}} G_{12}(r, z; r', z') E_2(r', z') \cdot \left(\frac{\sigma_f}{\sigma_0}(r', z') - 1\right) r' dr' dz' \quad (4)$$

When this equation is integrated over the probe coil we get the perturbed EMF. If we assume that the probe coil is uniformly and densely wound with n_c turns per unit area (in the r - z plane), we get for this EMF:

$$\text{EMF} = -2\pi n_c \iint_{\text{Probe Coil}} (E_0 - E_1) r dr dz \quad (5)$$

Finally, the electric field, E_0 , that is produced by the exciting coil is given by

$$\begin{aligned}
 E_0(r, z) &= -j\omega\mu_0 2\pi \iint_{\substack{\text{Exciting} \\ \text{Coil}}} G_{21}(r, z; r', z') J_0(r', z') r' dr' dz' \\
 &= -j\omega\mu_0 2\pi n_e I_0 \iint_{\substack{\text{Exciting} \\ \text{Coil}}} G_{21}(r, z; r', z') r' dr' dz' \quad , \quad (6)
 \end{aligned}$$

where J_0 is the exciting coil current density, n_e is the density of turns in the exciting coil, and I_0 is the current carried by the coil.

Equations (3)-(6) constitute the model system. The algorithm for using the system consists of first computing the incident field, E_0 , at the flaw, by (6); this is the right-hand side of (3). For a given distribution of flaw conductivity, $\sigma_f(r, z)$, (3) can be solved numerically. Its solution, the electric field, E_2 , in the flawed region is the source term for (4), which produces the perturbed electric field at the probe coil in region 1. The integral of the perturbed electric field produces the perturbed EMF, (5), which is then compared with the measured EMF to determine if the assumed flaw conductivity, $\sigma_f(r, z)$, is "close" to the actual (though unknown) flaw conductivity. The problem is really nonlinear because (3) involves the product of two unknowns, $\sigma_f(r, z)$ and $E_2(r, z)$. Thus, some form of iteration is required, in which one starts with an assumed distribution for $\sigma_f(r, z)$, and then hopes to converge to a final acceptable value.

The discretization of the problem via the method of moments is based on the use of a mesh, as shown in Figure 1. In order to reduce (3) to an algebraic system, we expand $E_2(r, z)$ and $(\sigma_f/\sigma_0 - 1)$ in pulse functions that are defined with respect to this mesh:

$$E_2(r, z) = \sum_{j=1}^{N_c} E_j P_j(r, z) \quad (7a)$$

$$\left(\frac{\sigma_f}{\sigma_0}(r, z) - 1\right) = \sum_{j=1}^{N_c} \sigma_j P_j(r, z) \quad , \quad (7b)$$

where N_c is equal to the number of cells in the mesh, and $P_j(r, z)$ is the j th N_c pulse function, which is defined by

$$\begin{aligned}
 P_j(r, z) &= 1 \quad , \quad (r, z) \text{ in } j\text{th cell} \\
 &= 0 \quad , \quad \text{otherwise} \quad . \quad (8)
 \end{aligned}$$

The j th expansion coefficients, E_j , σ_j , are the constant values of the fields over the j th cell.

Because E_2 and $(\sigma_f/\sigma_0 - 1)$ have identical expansions in non-overlapping pulse functions, it follows that their product does also:

$$E_2(r, z) (\sigma_f(r, z)/\sigma_0 - 1) = \sum_{j=1}^{N_c} E_j \sigma_j P_j(r, z) \quad . \quad (9)$$

The discretized version of (3) and (6) is the vector-matrix equation

$$[\bar{A} + j\omega\mu_0\sigma_0\bar{G}]\bar{E} = \bar{F}; \quad (10)$$

while the discretized version of (4) and (5) is the vector-matrix equation

$$\overline{EMF} = \overline{T}[\overline{OE}] \quad . \quad (11)$$

The expressions for the matrices above and other detailed calculations can be found in [14].

NUMERICAL EXPERIMENTS AND RESULTS

The theory of inversion involves two components, a theoretical model that is based on a rigorous application of electromagnetic theory, and numerical algorithms that effectively implement least-squares theory. Each of these has been dealt with, and now we illustrate how the method works for the reconstruction of computer simulated flaws.

All numerical experiments were run in double precision on the PRIME 550-II and IBM 370 machines. The double precision data word on the PRIME occupies 64 bits, of which 47 are the mantissa and 16 the exponent. The effective precision is about 14 digits. The IBM double precision word has a 56 bit mantissa, which allows an effective precision of about 17 digits. Precisions such as these are required for meaningful computations, because the condition number of the Jacobian matrix is phenomenal--on the order of 10^{12} . Even with this large condition number, the computations produced excellent results; in the worst case the reconstructions were exact to at least three places on the PRIME, and five places on the IBM. This verifies that the algorithms in the LINPACK and MINPACK packages tend to work better in higher precision.

The physical system that was modeled is shown in Figure 1. It consists of a fixed exciting coil and a single probe coil that can be moved axially. This system is typical of a common flaw detection

scheme. The mesh on which the discretization is defined is also shown. It consists of six rows of ten cells, and spans the entire tube wall-thickness. The starting position of the probe coil is at the left edge of the mesh, and the final position is at the right edge. The probe coil is stepped through fifty equal intervals between these limits, thereby generating a total of 100 real and imaginary EMF values that are used in the least-squares inversion.

The physical parameters of the model are typical of real systems. The inner radius of the tube is 0.310", and the outer radius, 0.375". The length of the mesh is 0.50" in the z-direction, thereby giving a cell resolution of 0.05" by 0.011". The probe coil's inner radius is 0.05", outer radius 0.100", and its length is 0.50", the same as the mesh. The exciting coil is centered on the mesh in the z-direction (neither of these last two items is a requirement of the inversion method). The density of turns of the exciting coil is 2×10^6 turns/m, which is comparable to that of 20 gauge copper wire. The probe coil has an inner radius of 0.100", outer radius of 0.26", and a length of 0.250". Its turn density is 2×10^7 turns/m, which is comparable to 30 gauge copper wire. The tube conductivity is 3.5×10^7 , which is equal to the conductivity of aluminum, and the frequency of operation is 1kHz.

In Figure 2 we show a simulated flaw (the "original") at the top and its reconstructed version at the bottom. The real (R) and imaginary (I) parts of the perturbed EMF, as measured by the probe coil when it is moved across the mesh, are shown in the middle of the figure. This EMF curve is actually an interpolation based on the fifty probe coil positions. In this figure, and the next two, we simulate the flaw by letting $\sigma_f = 0$ at the flaw location, and $\sigma_f = \sigma_0$ off of the flaw. Thus, according to (7)(b), $\sigma_j = -1$ if the jth cell lies on the flaw, and $\sigma_j = 0$, otherwise.

Note, in Figure 2, that because the original flaw is placed symmetrically in the mesh, the EMF is symmetrical about the center of the mesh, also. The reconstruction is clearly perfect (to at least three significant digits), indicating that the least-squares inversion algorithms work quite well in this model. We must be careful to note, however, that in Figures 2-6 we have considered only original flaws that are defined on the same mesh as that used for reconstruction; i.e., each part of the flaw is constant over a full cell of the reconstruction mesh. We consider the more general case, in which the flaw may be defined on a different mesh than that used for reconstruction (say, one with smaller cells, or cells that are displaced from the cells of the reconstruction mesh) in Figures 7, 8. This will test the ability of the model to resolve, as well as invert, data.

To satisfy ourselves that the excellent results that were obtained in Figure 2 were not due to symmetry, we considered the asymmetrical flaws of Figures 3 and 4. Again, the reconstruction was

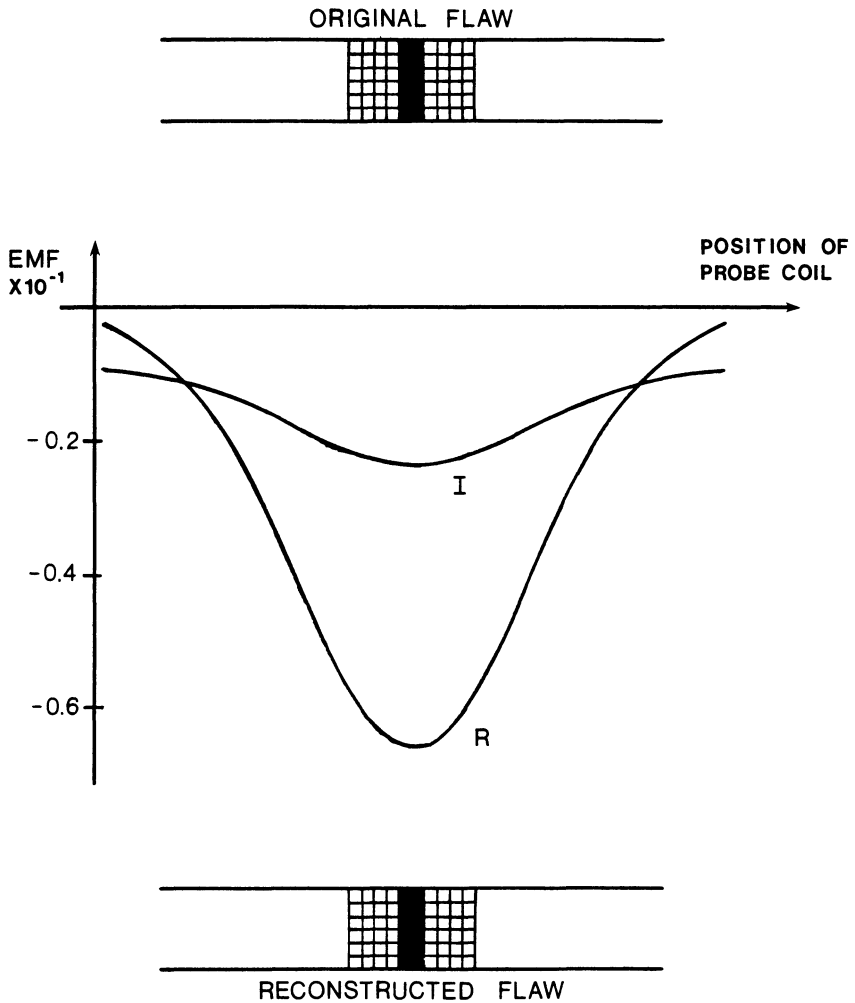


Figure 2. Illustrating a symmetrically placed flaw (top), the real (R) and imaginary (I) parts of the EMF induced into the probe coil (center), and the reconstructed flaw (bottom). The flaw consists of the darkened cells. The reconstruction is exact to at least three significant digits.

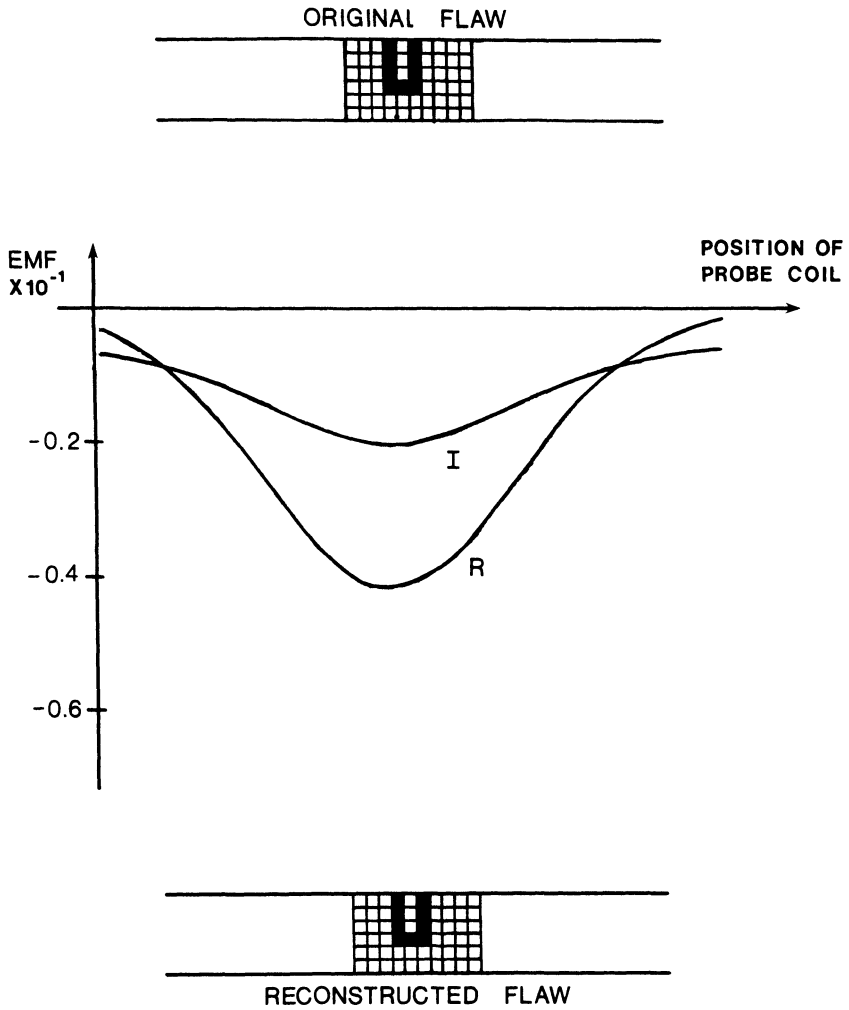


Figure 3. Illustrating the reconstruction of an asymmetrically placed flaw. The interpretation of the figure is the same as of Figure 2.

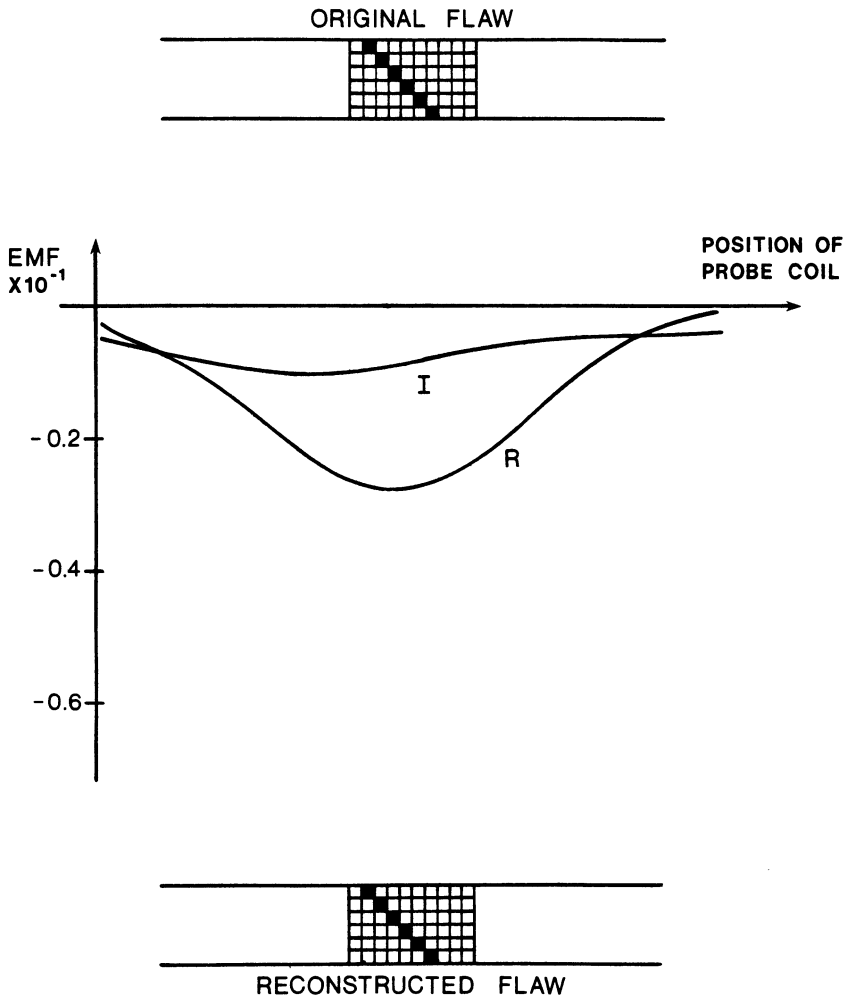


Figure 4. Illustrating the reconstruction of another asymmetrically placed flaw.

perfect to at least three significant digits. It should be noted from these three examples that the more concentrated the flaw, the greater is the peak of the EMF curve.

A crucial test of inversion in highly ill-conditioned systems has to do with corrupted data. The question is, does the reconstruction "follow" the corrupted data, or does the result lose all significant figures? In order to test our model's response to corrupted data, we performed the following numerical experiment. We assigned to each cell in the mesh a number between 0 and 1, chosen at random by using the FORTRAN random number generator. Then the model EMF that is produced by this "flaw" is computed. This "true" data is then corrupted by adding to it the same data multiplied by either 0.01, 0.10, or 0.20, and then using this as the "measured" EMF. Figure 5 shows the results of this experiment. There we show the original flaw, consisting of the sixty randomly chosen cell conductivities, followed by the reconstructed flaw, simulated by the sixty values of computed cell conductivities, for the case of 1%, 10%, and 20% corrupted data.

Again, the results are excellent. We don't, of course, expect to reconstruct the original flaw by using corrupted EMF data. We are happy, though, to see that the reconstructed flaw "tracks" the original flaw, in the sense that it departs by almost exactly 1%, 10%, or 20% from the original. Such stability in the face of a very ill-conditioned system attests to the excellence of the LINPACK and MINPACK algorithms.

The same results that are shown in Figures 2-5, are obtained with either the linear or nonlinear algorithms. The reason for this is that in (10) the term involving the matrix \underline{G} is much smaller than the first term, \underline{A} . Thus, the solution of the equation is $E \approx E_0$, and when this is substituted into (11) we see that the Jacobian matrix is constant, so that the nonlinear algorithms may be replaced by the simpler linear ones.

Our inversion method was also tested in the presence of a known irregularity. The case we present is where there is a notch. The results are presented in Figure 6.

When we generated and reconstructed on different grids, the nonlinear least-squares algorithms were no longer adequate. In this case it was important to impose the proper constraints on the σ_{ij} . Thus when we used the nonlinear programming routine VMCON [15], we got the results shown in Figures 7 and 8. VMCON uses the variable metric constraint method of Powell.

The results of the numerical experiments have been very good and suggest that the method can be used as the basis for the development of an engineering prototype system.

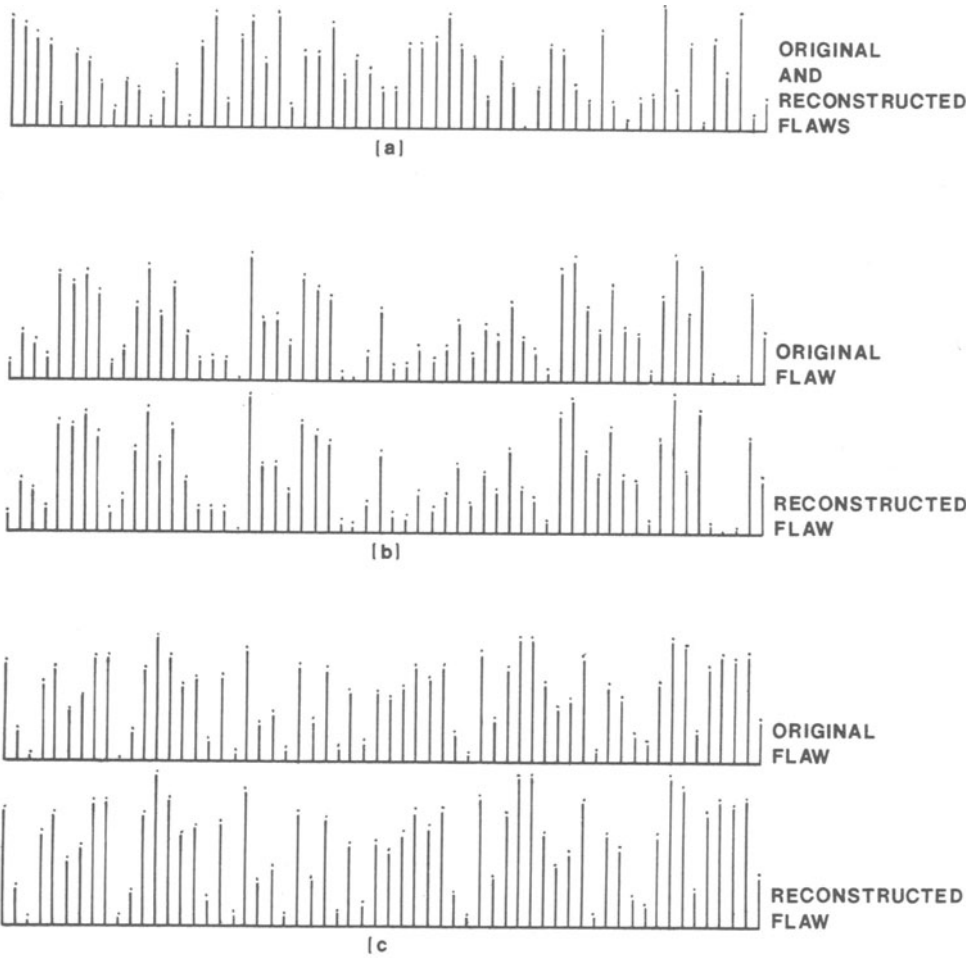


Figure 5. Illustrating the reconstruction of random flaws with perturbed EMF data: (a) 1% perturbation, (b) 10% perturbation, (c) 20% perturbation.

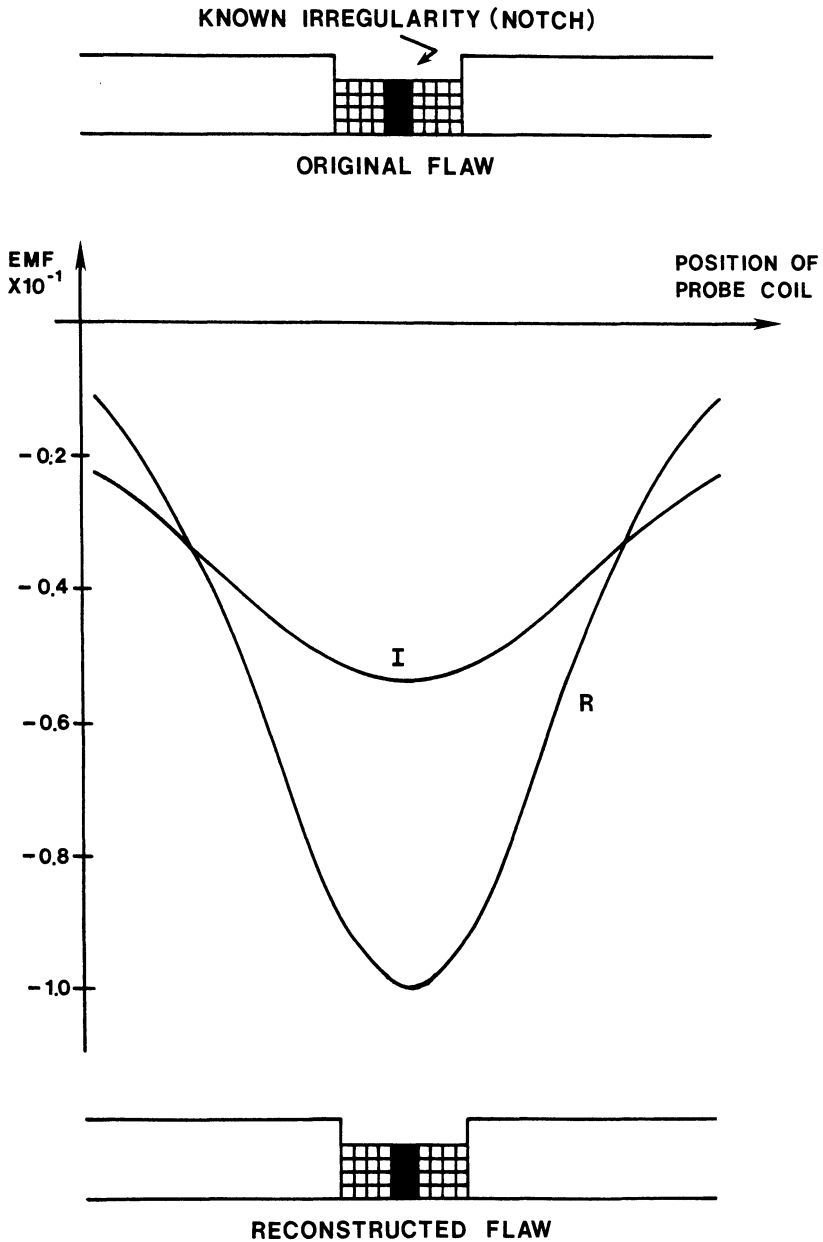
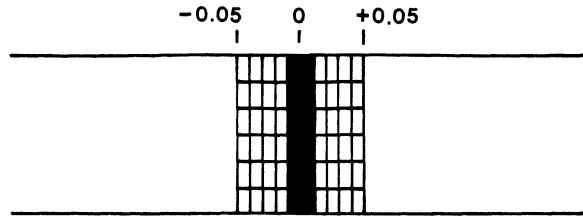
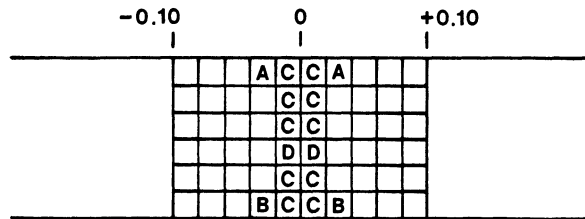


Figure 6. Illustrating the reconstruction of a flaw in the presence of a known irregularity (notch).



ORIGINAL FLAW AND GRID



RECONSTRUCTED FLAW AND GRID

A= -0.024
 B= -0.086
 C= -0.500
 D= -0.389

Figure 8. Illustrating the reconstruction of a flaw that was generated on a finer grid. The reconstruction grid is two times as wide as the generation grid.

REFERENCES

- [1] Special Issue on Inverse Methods in Electromagnetics, IEEE Transactions on Antennas and Propagation, Vol. AP-29, No. 2, March 1981.
- [2] P. C. Sabatier, ed., Applied Inverse Problems, Vol. 85, Lecture Notes in Physics, Springer-Verlag, Berlin, 1978.
- [3] H. P. Baltès, ed., Inverse Scattering Problems in Optics, Vol. 20, Topics in Current Physics, Springer-Verlag, Berlin, 1980.
- [4] W. E. Glenn, J. Ryu, S. H. Ward, W. J. Peeples and R. J. Phillips, "The Inversion of Vertical Magnetic Dipole Sounding Data," Geophysics, 38, No. 6 (Dec. 1973), pp. 1109-1129.
- [5] J. R. Inman, Jr., J. Ryu and S. H. Ward, "Resistivity Inversion," Geophysics, 38, No. 6 (Dec. 1973), pp. 1088-1108.
- [6] D. D. Jackson, "Interpretation of Inaccurate, Insufficient and Inconsistent Data," Geophys. J. R. Astr. Soc. (1972) 28, pp. 97-109.
- [7] D. L. B. Jupp and K. Vozoff, "Stable Iterative Methods for the Inversion of Geophysical Data," Geophys. J. R. Astr. Soc. (1975) 42, pp. 957-976.
- [8] M. L. Oristaglio and M. H. Worthington, "Inversion of Surface and Borehole Electromagnetic Data for Two-Dimensional Electrical Conductivity Models," Geophysical Prospecting, 1980, 28, 633-657.
- [9] S. H. Ward, W. J. Peeples and J. Ryu, "Analysis of Geoelectromagnetic Data," in Methods in Computational Physics, Geophysics, 13, 163-236.
- [10] P. Weidelt, "Inversion of Two-Dimensional Conductivity Structures," Physics of the Earth and Planetary Interiors, 10 (1975), 282-291.
- [11] Special Issue on Applications of Electromagnetic Theory to Geophysical Exploration, Proc. IEEE, Vol. 67, No. 7, July 1979.
- [12] J. J. Dongarra, J. R. Bunch, C. B. Moler and G. W. Stewart, LINPACK Users' Guide, Society for Industrial and Applied Mathematics, Philadelphia, 1979.
- [13] Jorge J. More, Burton S. Garbow and Kenneth E. Hillstom, "User Guide for MINPACK-1," Report No. ANL-80-74, Argonne National Laboratory, 9700 South Cass Avenue, Argonne, IL 60439, August 1980.
- [14] H. A. Sabbagh and L. D. Sabbagh, "Development of a System to Invert Eddy-Current Data and Reconstruct Flaws," Final Report: Contract No. N60921-81-C-0302 with Naval Surface Weapons Center [Code R34], White Oak Labs, Silver Springs, MD 20910, 18 June 1982.
- [15] R. L. Crane, K. E. Hillstom, and M. Minkoff, "Solution of the General Nonlinear Programming Problem with Subroutine VMCON," ANL-80-64, Argonne National Laboratory, 9700 South Cass Avenue, Argonne, IL 60439, July 1980.

DISCUSSION

E.K. Miller (Lawrence Livermore National Laboratory): It seems almost startling that the range of the matrix can be so ill-conditioned and yet seem so insensitive to noise and the data. Do you have any explanation for why this is so?

D.L. Sabbagh (Analytics, Inc.): No, I don't.

H.A. Sabbagh (Analytics, Inc.): I can't answer precisely, but my guess is that in the least squares process, you never invert a matrix. You consistently use QRD compositions and factorizations. I think that is a system that apparently maintains this sort of stability. The matrices are so ill-conditioned that you don't even talk about inverting them. Now we did note the following: When we ran it on my prime 550 in double precision (the prime maintains 47 to 48 bits of mantissa, and gives you 16 bits in the exponent), we were accurate to at least 3 decimal places and generally much better than that. When David ran it on his IBM 370, which maintains almost 56 bits, which corresponds to perhaps 17 decimal digits, he got 3 to 4 digits more. The Minpac routine is coded in such a way that you expect to get better efficiency with better precision. But, to answer the first part of the question, my guess is that it simply has to do with using the factorizations and all that QRD composition.

D.L. Sabbagh: You never solve a least squares problem by solving the normal equations, and you never find the generalized inverse. You do the QRD composition. That's the numerical way to do them. And the Minpac routine is an implementation of the Levenberg Marcoray algorithm that is very good.

H.A. Sabbagh: We found out one other thing: When we try to generate and reconstruct on different grids, it all worked very well. When we reconstructed and generated on the same grid, we were able to reconstruct perfectly. When we did it on opposite grids, the Minpac didn't work at all, and that's when we decided we finally had to use correct constraints. Everything was unconstrained at that point. When we constrained the normalized conductivity to lie between the correct values, everything fell into place and the last results that David showed you used a constrained programming.

D.L. Sabbagh: Not only programming, but also a variable metric method.